

Supplementary Material for
Gas-Phase and Solid-State Electronic Structure Analysis and DFT Benchmarking of HfCO

Isuru R. Ariyaratna¹, Yeongsu Cho¹, Chenru Duan^{1,2}, and Heather J. Kulik^{1,2*}

¹*Department of Chemical Engineering, Massachusetts Institute of Technology, Cambridge, MA 02139*

²*Department of Chemistry, Massachusetts Institute of Technology, Cambridge, MA 02139*
*email: hjkulik@mit.edu, phone: 617-253-4584

Contents

Figure S1 Interaction of CO molecule with Hf surface	Page S2
Figure S2 vbL diagram for states of HfCO	Page S2
Figure S3 Dissociation energy of HfCS with DFT	Page S3
Figure S4 Dissociation energy of HfCSe with DFT	Page S4
Table S1 Dissociation energy of HfCO with DFT	Page S5
Table S2 Dissociation energy of HfCS with DFT	Page S6
Table S3 Dissociation energy of HfCSe with DFT	Page S7
Figure S5 Dissociation energy of HfCX vs. dipole moment of the CX with DFT	Page S8
Table S4 Triplet-Quartet energy gap of HfCO with DFT	Page S9
Table S5 Ionization energy of HfCO with DFT	Page S10

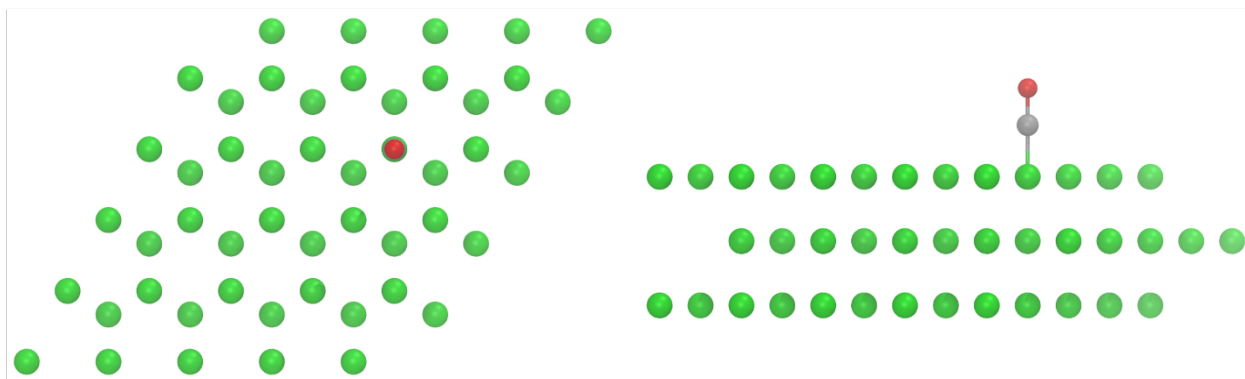


Figure S1. Geometry of CO molecule on periodic (001) surface of hexagonal Hf optimized with the BLYP functional. The C atom is 2.22 Å from the Hf surface and C-O bond length is 1.17 Å.

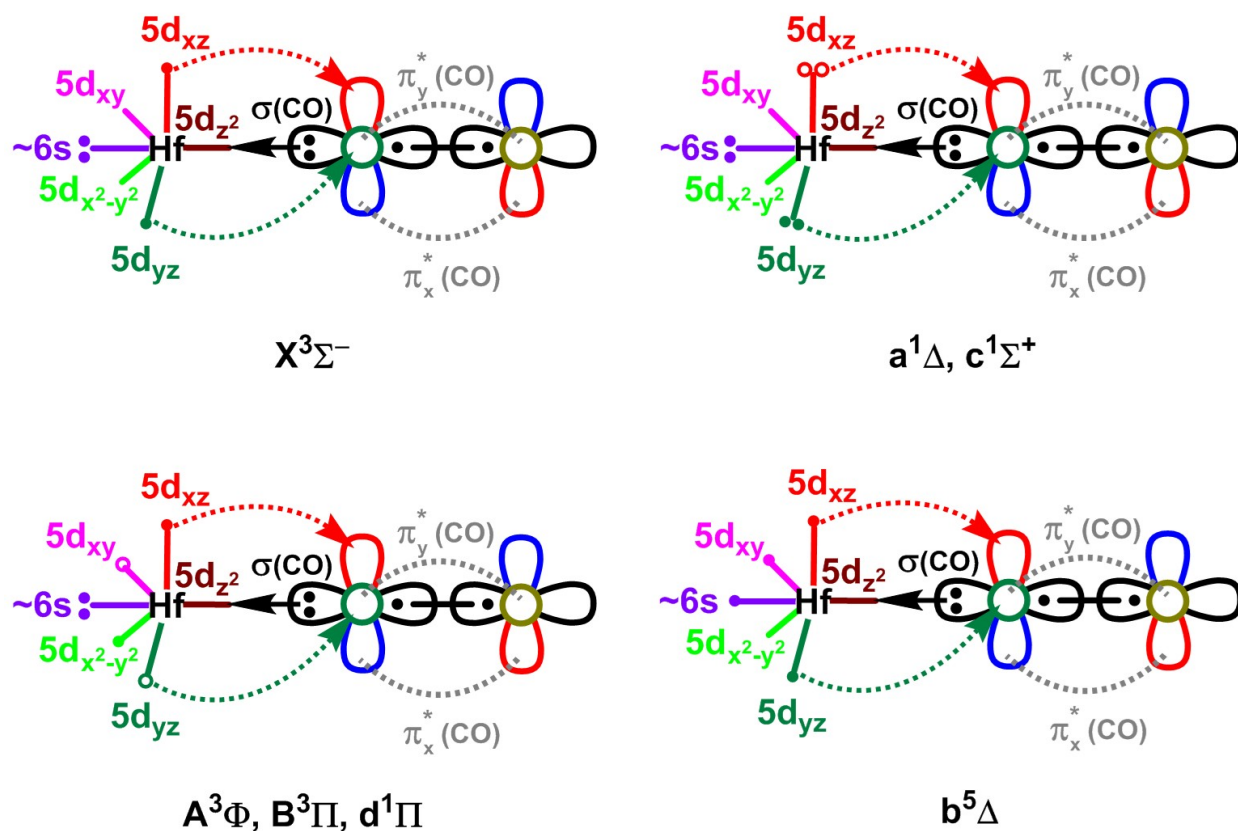


Figure S2. Proposed valence-bond-Lewis (vbl) diagrams for the seven lowest electronic states of HfCO. The π_x and π_y bonds of CO are omitted for clarity. The two $5d_{xz}$ and $5d_{yz}$ electrons of $X^3\Sigma^-$ have the same spin. The multireference $(1\pi_x)^2 \pm (1\pi_y)^2$ components of the $a^1\Delta$ and $c^1\Sigma^+$ states are shown by electron pairs with open and solid circles. Similarly, the π^1d^1 electron combinations of $A^3\Phi$, $B^3\Pi$, and $d^1\Pi$ are depicted in open and solid circles. See main text Table 1 for more details on electronic configurations.

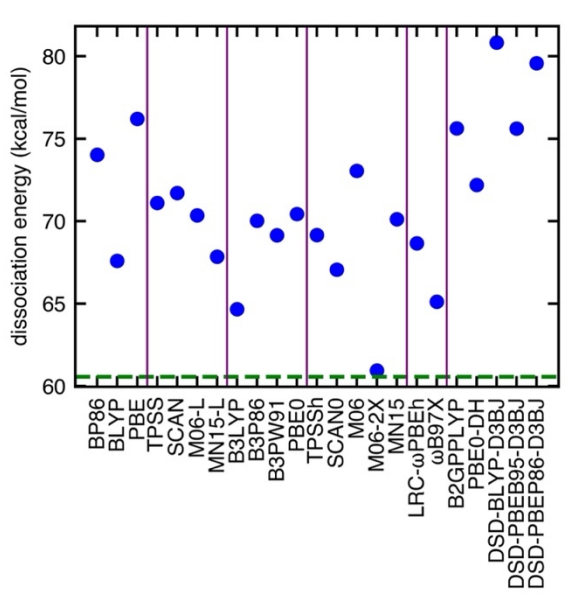


Figure S3. Dissociation energy (D_e , in kcal/mol) of HfCS calculated with different DFT functionals using the def2-QZVP basis set (blue dots). Each class of density functionals is separated with vertical purple lines and ordered by the rung on Jacob's ladder (left to right: GGA, meta-GGA, global GGA hybrid, meta-GGA hybrid, range-separated hybrid, and double hybrid). The horizontal green dashed line represents the CCSD(T)/TZ dissociation energy of HfCS.

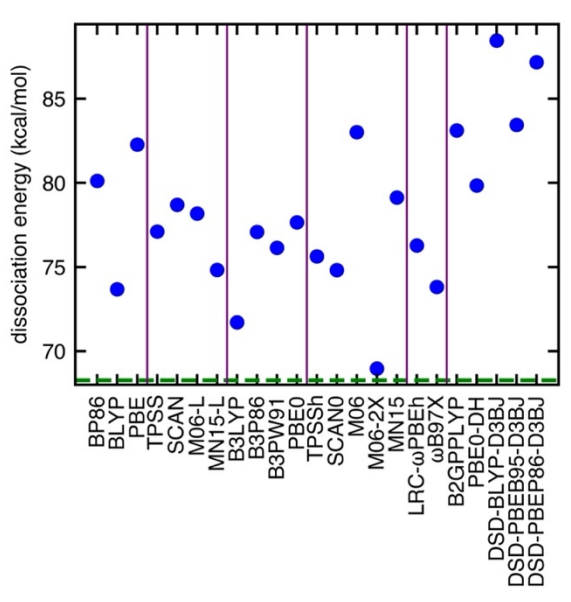


Figure S4. Dissociation energy (D_e , in kcal/mol) of HfCSe calculated with different DFT functionals using the def2-QZVP basis set (blue dots). Each class of density functionals is separated with vertical purple lines and ordered by the rung on Jacob's ladder (left to right: GGA, meta-GGA, global GGA hybrid, meta-GGA hybrid, range-separated hybrid, and double hybrid). The horizontal green dashed line represents the CCSD(T)/TZ dissociation energy of HfCSe.

Table S1. Dissociation energy (D_e) of HfCO (kcal/mol) calculated with different DFT functionals using the def2-QZVP basis set and % DFT D_e error with respect to the CCSD(T)-A5Z D_e (29.96 kcal/mol).

	DFT functional	D_e	% DFT error
GGA	BP86	41.37	38.07
	BLYP	35.02	16.87
	PBE	43.19	44.17
meta-GGA	TPSS	38.59	28.81
	SCAN	38.60	28.84
	M06-L	37.07	23.74
	MN15-L	36.95	23.34
hybrid	B3LYP	31.07	3.72
	B3P86	36.35	21.33
	B3PW91	35.46	18.37
	PBE0	36.35	21.34
meta-GGA hybrid	TPSSh	36.11	20.54
	SCAN0	32.83	9.57
	M06	38.38	28.11
	M06-2X	27.62	-7.81
	MN15	38.56	28.72
range-separated hybrid	LRC- ω PBEh	35.24	17.62
	ω B97X	30.24	0.95
double hybrid	B2GP-PLYP	40.61	35.53
	PBE0-DH	37.39	24.81
	DSD-BLYP-D3BJ	45.32	51.27
	DSD-PBEB95-D3BJ	40.63	35.61
	DSD-PBEP86-D3BJ	44.69	49.18

Table S2. Dissociation energy (D_e) of HfCS (kcal/mol) calculated with different DFT functionals using the def2-QZVP basis set and % DFT D_e error with respect to the CCSD(T)-TZ D_e (60.58 kcal/mol).

	DFT functional	D_e	% DFT error
GGA	BP86	74.02	22.19
	BLYP	67.60	11.59
	PBE	76.20	25.79
meta-GGA	TPSS	71.11	17.38
	SCAN	71.71	18.38
	M06-L	70.35	16.13
	MN15-L	67.85	12.01
hybrid	B3LYP	64.66	6.74
	B3P86	70.03	15.60
	B3PW91	69.14	14.14
	PBE0	70.43	16.26
meta-GGA hybrid	TPSSh	69.16	14.16
	SCAN0	67.06	10.70
	M06	73.05	20.59
	M06-2X	60.95	0.61
	MN15	70.13	15.76
range-separated hybrid	LRC- ω PBEh	68.66	13.34
	ω B97X	65.12	7.49
double hybrid	B2GP-PLYP	75.63	24.84
	PBE0-DH	72.20	19.18
	DSD-BLYP-D3BJ	80.83	33.43
	DSD-PBEB95-D3BJ	75.61	24.82
	DSD-PBEP86-D3BJ	79.57	31.35

Table S3. Dissociation energy (D_e) of HfCSe (kcal/mol) calculated with different DFT functionals using the def2-QZVP basis set and % DFT D_e error with respect to the CCSD(T)-TZ D_e (68.28 kcal/mol).

	DFT functional	D_e	% DFT error
GGA	BP86	80.12	17.34
	BLYP	73.68	7.91
	PBE	82.28	20.50
meta-GGA	TPSS	77.11	12.94
	SCAN	78.70	15.26
	M06-L	78.17	14.49
	MN15-L	74.83	9.60
hybrid	B3LYP	71.72	5.04
	B3P86	77.09	12.90
	B3PW91	76.15	11.53
	PBE0	77.66	13.74
meta-GGA hybrid	TPSSh	75.64	10.78
	SCAN0	74.82	9.57
	M06	83.01	21.57
	M06-2X	68.97	1.02
	MN15	79.13	15.89
range-separated hybrid	LRC- ω PBEh	76.28	11.72
	ω B97X	73.82	8.12
double hybrid	B2GP-PLYP	83.12	21.73
	PBE0-DH	79.84	16.93
	DSD-BLYP-D3BJ	88.46	29.55
	DSD-PBEB95-D3BJ	83.45	22.22
	DSD-PBEP86-D3BJ	87.17	27.67

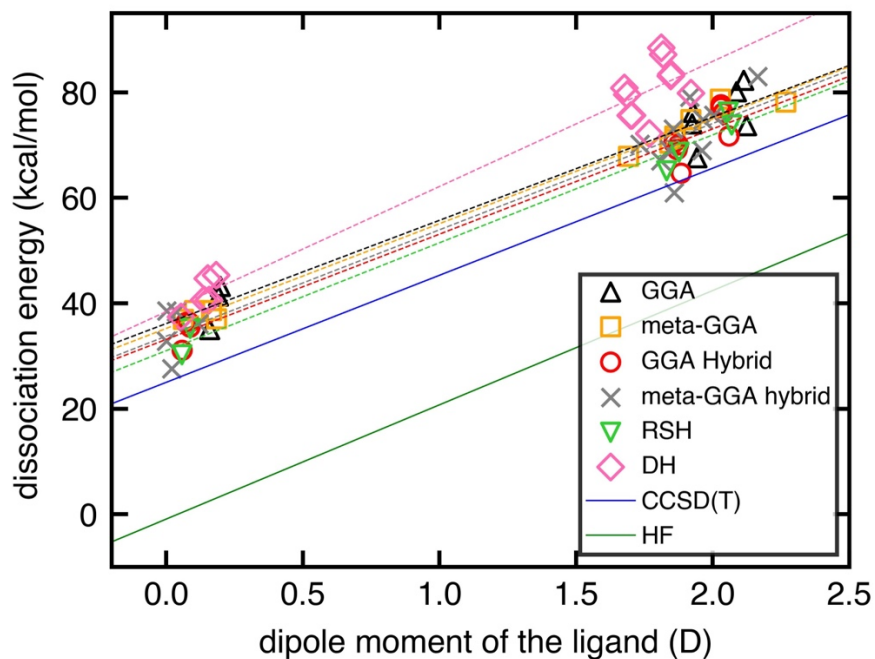


Figure S5. Dissociation energy (D_e , in kcal/mol) of HfCX vs. dipole moment (μ , in D) of the CX for $X = \text{O}, \text{S}, \text{Se}$ computed with different DFT functionals using the def2-QZVP basis set (trendlines of different functionals are depicted in dashed lines). The trendlines of HF/cc-pVTZ(-PP) and CCSD(T)/cc-pVTZ(-PP) are shown in green and blue solid lines with the $y = 21.66x - 0.92$ ($R^2 = 0.97$) and $y = 20.30x + 25.01$ ($R^2 = 0.99$) fittings, respectively. Trendlines of GGA, meta-GGA, GGA Hybrid, meta-GGA hybrid, RSH, and DH are $y = 19.58x + 36.16$ ($R^2 = 0.95$), $y = 19.86x + 35.23$ ($R^2 = 0.99$), $y = 19.96x + 33.16$ ($R^2 = 0.98$), $y = 20.17x + 33.77$ ($R^2 = 0.94$), $y = 20.46x + 31.02$ ($R^2 = 0.98$), and $y = 23.73x + 38.42$ ($R^2 = 0.96$), respectively.

Table S4. Triplet-Quintet energy gap (ΔE_{T-Q}) of HfCO (kcal/mol) calculated with different DFT functionals using the def2-QZVP basis set and % DFT ΔE_{T-Q} error with respect to CCSD(T)-TZ ΔE_{T-Q} (22.36 kcal/mol).

	DFT functional	ΔE_{T-Q}	% DFT error
GGA	BP86	12.74	-43.02
	BLYP	17.70	-20.85
	PBE	11.41	-48.95
meta-GGA	TPSS	9.35	-58.19
	SCAN	4.46	-80.06
	M06-L	22.49	0.60
	MN15-L	19.32	-13.59
hybrid	B3LYP	16.91	-24.37
	B3P86	12.85	-42.55
	B3PW91	9.61	-57.03
	PBE0	10.32	-53.83
meta-GGA hybrid	TPSSh	9.43	-57.83
	SCAN0	5.81	-74.03
	M06	36.53	63.40
	M06-2X	21.47	-3.96
	MN15	28.24	26.28
range-separated hybrid	LRC- ω PBEh	10.29	-53.98
	ω B97X	31.81	42.27
double hybrid	B2GP-PLYP	20.10	-10.11
	PBE0-DH	11.72	-47.56
	DSD-BLYP-D3BJ	21.07	-5.76
	DSD-PBEB95-D3BJ	21.97	-1.73
	DSD-PBEP86-D3BJ	20.71	-7.36

Table S5. Adiabatic ionization energy (IE) of HfCO (eV) calculated with different DFT functionals using the def2-QZVP basis set and % DFT IE error with respect to CCSD(T)-TZ IE (6.974 eV).

	DFT functional	IE	% DFT error
GGA	BP86	7.146	2.47
	BLYP	7.056	1.18
	PBE	7.003	0.42
meta-GGA	TPSS	6.871	-1.48
	SCAN	6.813	-2.31
	M06-L	7.141	2.39
	MN15-L	7.219	3.51
hybrid	B3LYP	7.095	1.74
	B3P86	7.169	2.79
	B3PW91	6.879	-1.36
	PBE0	6.853	-1.74
meta-GGA hybrid	TPSSh	6.832	-2.04
	SCAN0	6.760	-3.06
	M06	7.547	8.22
	M06-2X	7.176	2.89
	MN15	7.354	5.45
range-separated hybrid	LRC- ω PBEh	6.780	-2.78
	ω B97X	7.333	5.14
double hybrid	B2GP-PLYP	7.011	0.54
	PBE0-DH	6.837	-1.97
	DSD-BLYP-D3BJ	7.023	0.70
	DSD-PBEB95-D3BJ	6.941	-0.48
	DSD-PBEP86-D3BJ	7.025	0.74